THE ASTRONOMICAL JOURNAL VOLUME 107, NUMBER 3 MARCH 1994

RADIO IMAGING OF TWO SUPERNOVA REMNANTS CONTAINING PULSARS

D. A. FRAIL
National Radio Astronomy Observatory, P.O. Box O, Socorro, New Mexico 87801-0387
Electronic mail: dfrail@nrao.edu

N. E. KASSIM
Remote Sensing Division, Naval Research Laboratory
Electronic mail: kassim@rira.nrl.navy.mil

K. W. WEILER
Remote Sensing Division, Naval Research Laboratory
Electronic mail: kweiler@shimmer.nrl.navy.mil

Received 1993 July 20; revised 1993 November 4

ABSTRACT

The supernova remnants G 5.4−1.2 and G 8.7−0.1 each have a 15 000 yr old pulsar projected along their outside edges. If these are true pulsar-supernova remnant associations then the implied pulsar transverse motions for PSR1757−24 and PSR 1800−21 are excessively large (1500–2500 km s^{-1}). We present new radio observations made at the VLA in the continuum at 327 MHz and the H I line at 1420 MHz to address this issue. For G 5.4−1.2 we better constrain the true extent of the remnant and its shape. We also derive an H I absorption distance and the spectral index distribution across the bright western side of the remnant. All the available evidence suggests that G 5.4−1.2 and PSR 1757-24 are associated. Our deep 327 MHz image of G 8.7−0.1 reveals faint extensions of the remnant but no new emission is seen near PSR 1800−21. A possible new supernova remnant is also discovered north of G 8.7−0.1. Several difficulties are presented for the proposed association between G 8.7−0.1 and PSR 1800−21, the most serious of which are the lack of a pulsar-powered nebula and the discrepant distance estimates for the pulsar and supernova remnant. We conclude that PSR 1800−21 is a foreground object, unrelated to G 8.7−0.1.

1. INTRODUCTION

In recent years the number of known pulsar–supernova remnant associations has continued to grow, but the total number is only about 12 (Bailes & Johnston 1993). These associations, by being so few in number and by their often very unusual characteristics, continue to surprise us. They challenge established notions concerning the origin of neutron stars, the evolution of supernova remnants (SNRs), and the role that pulsars play in this evolution. In particular, two notable associations have raised new questions: G 5.4−1.2 with PSR 1757−24 (Frail & Kulkarni 1991; Manchester *et al.* 1991), and G 8.7−0.1 with PSR 1800−21 (Kassim & Weiler 1990a).

1.1 SNR G 5.4−1.2 and PSR 1757−24

The true nature of G 5.4−1.2 has been a source of considerable controversy over the years. Helfand & Becker (1985) proposed that G 5.4−1.2, nicknamed "The Duck," belonged to a whole new class of accretion-powered radio sources. They were struck by its axially symmetric morphology; the brightest arc of the remnant is joined at its center by a bulge of emission to a compact source (G 5.27−0.9). Weiler & Sramek (1988), however, disputed the interpretation of Helfand & Becker and argued that G 5.4−1.2 was just an unusual SNR. When Caswell *et al.* (1987) imaged the remnant at 843 MHz with the Molonglo Observatory Synthesis Telescope (MOST), they found a faint radio arc to the east of G 5.4−1.2 that appeared to be the limb brightened eastern edge of a normal SNR with roughly circular symmetry. Caswell *et al.* further speculated that the pulsar PSR 1757−24, found by Manchester *et al.* (1985), was embedded in G 5.27−0.9 and was exciting the remnant. Frail & Kulkarni (1991) and Manchester *et al.* (1991) confirmed this speculation by pinpointing the location of the pulsar on the western edge of G 5.27−0.9. The young age for the pulsar (16 000 yr), the similar distances for PSR 1757−24 and G 5.4−1.2, and the apparent bridge of emission linking the remnant with the pulsar are the bases for arguing for a real physical association between these two objects (Frail & Kulkarni 1991).

1.2 SNR G 8.7−0.1 and PSR 1800−21

The nature of G 8.7−0.1 (W30) has also been a source of mystery. In particular, its radio morphology is ill-defined: bright, compact H II regions are superimposed upon a large (45′) amorphous, nonthermal region of low surface brightness [$\Sigma(1\ \mathrm{GHz}) = 5.7\times10^{-21}$ W m^{-2} Hz^{-1} sr^{-1}]. Odegard (1986) and Kassim & Weiler (1990b) clearly established that G 8.7−0.1 was a SNR, measuring a nonthermal spectral index for the extended emission of $\alpha = -0.53$ (where $S_\nu \propto \nu^{+\alpha}$). G 8.7−0.1 appears to be a SNR in a star-forming region. The young pulsar PSR

 0004-6256/94/107(3)/1120/8/$0.90

Report Documentation Page

Form Approved
OMB No. 0704-0188

1. REPORT DATE	2. REPORT TYPE	3. DATES COVERED
MAR 1994		**00-00-1994 to 00-00-1994**

4. TITLE AND SUBTITLE	5a. CONTRACT NUMBER
Radio Imaging of Two Supernova Remnants Containing Pulsars	5b. GRANT NUMBER
	5c. PROGRAM ELEMENT NUMBER
6. AUTHOR(S)	5d. PROJECT NUMBER
	5e. TASK NUMBER
	5f. WORK UNIT NUMBER
7. PERFORMING ORGANIZATION NAME(S) AND ADDRESS(ES) **Naval Research Laboratory,Code 7213,4555 Overlook Avenue, SW,Washington,DC,20375**	8. PERFORMING ORGANIZATION REPORT NUMBER
9. SPONSORING/MONITORING AGENCY NAME(S) AND ADDRESS(ES)	10. SPONSOR/MONITOR'S ACRONYM(S)
	11. SPONSOR/MONITOR'S REPORT NUMBER(S)

12. DISTRIBUTION/AVAILABILITY STATEMENT
Approved for public release; distribution unlimited

13. SUPPLEMENTARY NOTES

14. ABSTRACT

15. SUBJECT TERMS

16. SECURITY CLASSIFICATION OF:			17. LIMITATION OF ABSTRACT	18. NUMBER OF PAGES	19a. NAME OF RESPONSIBLE PERSON
a. REPORT **unclassified**	b. ABSTRACT **unclassified**	c. THIS PAGE **unclassified**		**10**	

1800−21 is located near the southwestern edge of G 8.7 −0.1; it lies in a faint extension of the remnant first seen by Kassim & Weiler (1990b). Kassim & Weiler (1990a) argued that PSR 1800−21 is physically associated with G 8.7−0.1 on the basis of its location, its young age (16 000 yr) and the fact that the best available distance for both objects agreed.

1.3 Pulsar Velocities

Despite the evidence in favor of these associations, some uncertainty remains. The most unsettling feature of both associations are the high space velocities apparently required for the pulsars. In each case the pulsar is found well away from the geometric center of its supernova remnant. If the pulsars were born at the geometric center of their remnants, then we infer pulsar transverse velocities on the order of 2500 km s^{-1} for PSR 1757−24 and 1700 km s^{-1} for PSR 1800−21; well above the average measured pulsar velocities of 100–200 km s^{-1} (Lyne *et al.* 1982) and exceeding the maximum transverse velocity ever measured of 1000 km s^{-1} (for PSR 2224+65) (Harrison *et al.* 1993).

Such high velocities cannot be produced by the angular momentum imparted to the neutron star in the breakup of a close binary (Dewey & Cordes 1987). Clearly some sort of asymmetry at the time of the SN explosion would be required to provide the velocity "kick." Several mechanisms have been proposed (Woosley 1987; Abramovici *et al.* 1992; Burrows & Fryxell 1992) but even then the degree of asymmetry required to produce these high velocities is embarrassingly large, much larger than the 1–2% of the supernova's kinetic energy ($E_k \simeq 10^{51}$ ergs) which is commonly assumed (Woosley 1987). Pulsar proper motion measurements which are currently underway could help resolve this issue, but it should be noted that these high proposed velocities depend on two other poorly known quantities: (a) the point of origin for the supernova explosion (usually assumed to be the location of the geometric center of the remnant), and (b) the distance to the pulsar (or supernova remnant).

To address these questions and to test whether these PSR–SNR associations are real, we have initiated a study of these SNRs with the VLA.[1] Synthesis images at 327 MHz of G 5.4−1.2 and G 8.7−0.1 were made to enable us to better locate the geometric centers of the remnants, and 21 cm line observations of G 5.4−1.2 were made for the purpose of deriving a kinematic distance to the remnant.

2. OBSERVATIONS

The continuum observations were made with the VLA in the CnB (1992 February 9) and DnC (1992 June 6) hybrid array configurations. Two separate IF bands, each measuring both hands of circular polarization and each with a bandwidth of 3.125 MHz were used at 327.5 and 331.5 MHz. Each IF bandwidth was divided into 32 channels and the interference-free channels were selected and summed to form a final continuum database for further processing. All data reduction and calibration were done following standard practice in use at the VLA. The total integration time on each source is approximately 4 h.

The image fidelity at 327 MHz is limited not by system noise but by confusion from the myriad of background radio sources in the field. This is particularly true in the Galactic plane where there are numerous bright, extended sources such as H II regions and supernova remnants. In order to reduce the effect of the confusing sources, a wide field imaging algorithm was used, described by Cornwell (1993) and Cornwell & Perley (1992), which incorporates the deconvolution and self-calibration processes together. A large 6.5° field centered on each SNR was imaged by dividing it into 81 "patches." Each patch was CLEANed separately and all clean components were utilized in a model for self-calibration. Multiple clean/self-cal passes were made through the database until the residuals were reduced below a suitable level (Cornwell 1993). The final rms noise on our images is approximately 3 mJy $beam^{-1}$, about a factor of 10 above the limits reached by Cornwell (1993) for typical fields. However, given the extra contribution of the nonthermal background emission of the Galaxy to the system noise temperature at this frequency [$\simeq$400 K at 408 MHz: Haslam *et al.* (1982)], the noise limit we reached is close to the system noise limit.

The spectral line observations of G 5.4−1.2 were made in the hybrid DnC array on 1992 June 9. A bandwidth of 1.56 MHz was used in both left and right circular hands of polarization centered on the 21 cm line of neutral hydrogen shifted to a frequency corresponding to a velocity of +40 km s^{-1} relative to the Local Standard of Rest (V_{LSR}). A total of 256 channels were employed across this band, for a channel resolution of 6.1 kHz or 1.3 km s^{-1}. The total integration time on G 5.4−1.2 was 2.6 h.

The difficulties in obtaining accurate 21 cm absorption spectra against extended continuum sources are well known (cf. Frail & Clifton 1989). While data from the shortest baselines contain most of the flux from the extended source, they also contain significant extended H I emission which contaminates the absorption spectrum and complicates the interpretation of the profiles. Some care must be taken to choose a suitable short baseline limit to balance the need for significant continuum emission from the source under study but to discriminate against the local H I line emission. Fortunately, in the case of G 5.4−1.2 there are several point sources in the field to help with this problem. Absorption spectra for the point sources were formed with a variety of minimum baseline values to establish that at the optical depth values of interest there is little H I emission contaminating the spectra for baselines longer than 800 λ.

The continuum emission was subtracted from the dataset following the method of Cornwell *et al.* (1992) and a spectral cube was formed from this. Absorption spectra were taken at the brightest portions of G 5.4−1.2. Where an average spectrum was formed over an extended region,

[1]The Very Large Array is operated by the Associated Universities, Inc. under cooperative agreement with the National Science Foundation.

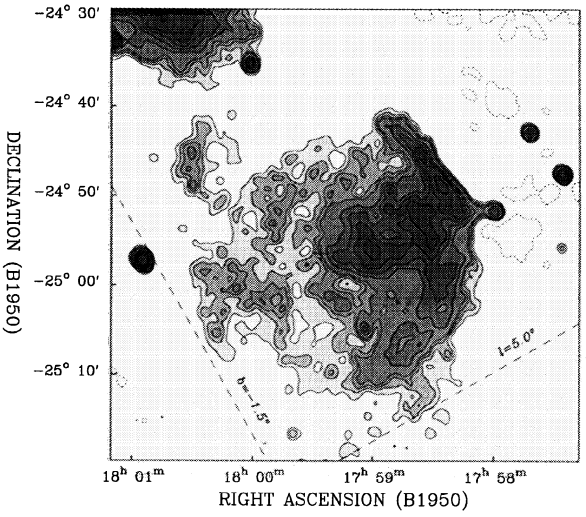

FIG. 1. A radio continuum image of the supernova remnant G 5.4−1.2 at 327 MHz. Uniform weighting was used and the synthesized beamsize is 73″×68″. Contour intervals are −5, 3, 5, 7, 9, 15, 20, 25, 30, 40 times 7.5 mJy beam^{-1}, with the negative contour shown with a dashed line. The approximate geometric center of the remnant is indicated by the cross. PSR 1757−24 lies within the pointlike extension on the western edge of G 5.4−1.2, 5′ to the north and 20.6′ to the west of the geometric center.

the data were weighted by the inverse square of the signal to noise at each point.

3. RESULTS

3.1 Continuum Images at 327 MHZ

SNR G 5.4−1.2 and PSR 1757−24. Figure 1 is a subsection from our wide field image, showing the region around G 5.4−1.2. All of the familiar features in the high resolution images of Caswell *et al.* (1987) and Becker & Helfand (1985) are visible. In addition, we see for the first time that the inner portion of the remnant is filled with weak, diffuse emission with a mean intensity of only 15 mJy beam^{-1}. Further, rather than the limb-brightened eastern shell seen by Caswell *et al.* (1987), we see a more amorphous structure. A lack of short spacings is the likely reason why Caswell *et al.* (1987) did not see these structures with the MOST at 843 MHz. Kassim (1991) also did not see the faint eastern shell in an early 327 MHz VLA image, but this can be attributed to the low sensitivity of the system at that time.

The remnant appears well confined and can be described by a simple circle with little or no ellipticity. A fit through the edge of the remnant enclosing most of the emission gives a radius for the circle of 15.5′, centered at $\alpha(1950) = 17^h\ 59^m26^s$ and $\delta(1950) = -24°\ 56'\ 30''$. We define this to be the geometric center of the remnant.

It is noteworthy that a line drawn through the pulsar and the "neck of the duck" lies nearly east–west and does not intersect the geometric center of the remnant. It misses it by nearly 5′ to the north. We will return to this point in Sec. 4.

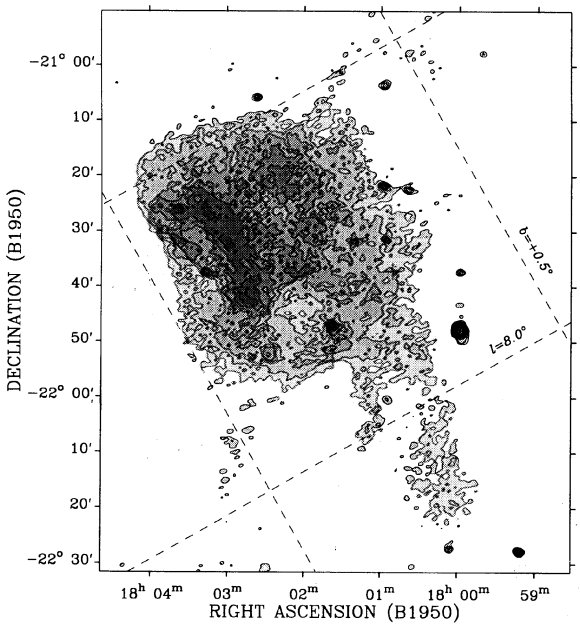

FIG. 3. A radio continuum image of the supernova remnant G 8.7−0.1 at 327 MHz. Uniform weighting was used and the synthesized beamsize is 55″×37″. Contour intervals are 10, 25, 50, 75, 100, 150, 200, 300, 400 mJy beam^{-1}. The position of PSR 1800−21 is indicated by the cross.

The image of the full field Fig. 2 [Plate 87] shows numerous radio sources including the H II regions M8 and W 28A and the SNR W28.

SNR G 8.7−0.1 and PSR 1800−21. Figure 3 shows the area in the immediate vicinity of G 8.7−0.1. The H II regions first imaged by Kassim & Weiler (1990b) are plainly visible. Striking new features in this image are the low surface brightness "plumes" emanating from the bounds of the remnant. They are most prominent on the southern and western edges of the remnant with surface brightnesses $\Sigma(0.3\ \text{GHz}) \simeq 2.3\times10^{-21}$ W m^{-2} Hz^{-1} sr^{-1}. There is also a 5′ cavity or "hole" within the remnant at $\alpha(1950) = 18^h02^m$, $\delta(1950) = -21°$ 45′, bounded by the H II regions C, D, and E (as defined by Kassim & Weiler 1990b) with little or no radio emission. The origin of either the hole or the plumes is unknown. PSR 1800−21, the young pulsar which is thought to possibly be associated with G 8.7−0.1, is too weak to be seen above the extended emission from the SNR.

The morphology of G 8.7−0.1 seems to defy classification. There is no clear shell structure, nor is it a "plerion" at least in the conventional sense. The center of G 8.7−0.1, set by Kassim & Weiler (1990b) at $\alpha(1950) = 18^h\ 02^m$, $\delta(1950) = -21°34'$, is at best a geometric definition. Given the complex morphology that the image reveals, there is no reason to believe that the geometric center is necessarily related to the blast center of the original supernova event. The total flux density of the W30 complex (SNR+H II regions) is 165 Jy. This is slightly higher than the value of 146 Jy obtained by Kassim & Weiler (1990b) from their VLA image but exactly the value they estimate from single dish surveys of this region.

Within the wide field image of the full field Fig. 4 [Plate 88] there are numerous H II regions, extragalactic point sources, and supernova remnants. In addition to known SNRs, G 8.7−0.1, W 28, G 10.0−0.3, G 11.2−0.3 and G 9.8+0.6, there is a possible new remnant G 9.7−0.1. Figure 5 is a subsection of our wide field image and shows that G 9.7−0.1 is a partial shell with a 15′ diameter, an average surface brightness of $\Sigma(0.3\ \mathrm{GHz}) = 10^{-21}$ W m^{-2} Hz^{-1} sr^{-1}, and total flux density of 1.5 Jy. Further observations, however, are required to confirm that the emission is nonthermal and that the source is, in fact, a SNR. It is not surprising that previous surveys of this area (Caswell 1983) missed such a low surface brightness source and it underscores the importance of low frequency surveys of the Galactic plane. Present radio catalogues of SNRs are deficient in small-diameter SNRs and extended, low surface brightness SNRs. The 327 MHz system at the VLA with the wide field imaging algorithms is most sensitive to the second type of remnants and could be used to great effect to search for these objects. For example, a recent 327 MHz survey with the Westerbork Synthesis Radio Telescope of a 46° strip ($b = \pm 1.5°$) of the Galactic plane resulted in a near doubling of the SNR population in the observed region (Taylor *et al.* 1992). We also note that the known pulsar PSR 1805−20 is visible in Fig. 5 as a 19 mJy point source.

3.2 H I Absorption Profiles for G 5.4−1.2

An absorption spectrum measured against the brightest continuum emission from G 5.4−1.2 is shown in Fig. 6 along with an emission spectrum in the same direction. An absorption spectrum for 1757−248, an extragalactic point source in the same field, is shown for comparison. We chose to form separate absorption spectra for the shell of G 5.4−1.2 and the compact nebula (the head of the duck) outside the remnant (G 5.27−0.9) which contains the pulsar. This allows us to test whether these two objects are at the same kinematic distance. The total flux density for 1757−248, the G 5.4−1.2 shell, and G 5.27−0.9 are 78, 35, and 240 mJy, respectively. The absorption spectrum for the shell of G 5.4−1.2 had to be smoothed with a three-bin boxcar to improve the signal to noise in the profile.

The method by which one determines a kinematic distance to a galactic object with H I emission and absorption spectra is well described in Frail & Weisberg (1990). Basically, a source is at least as far away as the distance corresponding to the radial velocity of the last absorption feature. In some circumstances an upper limit may also be derived if it can be established that there is a bright emission peak beyond this velocity against which we do not see the source in absorption. Converting these velocities to distances is done with the aid of a galactic rotation model.

The absorption spectra in Fig. 6 are remarkably similar. The deepest absorption lines at +7 and +13 km s^{-1} correspond to prominent self-absorption features appearing in the emission spectrum. The depth of the absorption is less for G 5.27−0.9 than it is for the other sources but this is likely due to the superior quality of its spectrum. The total widths of the absorption profiles are also similar. Absorption is detectable from 0 to +27 km s^{-1}. For G 5.27−0.9 this extends to 30 km s^{-1} and there may be weak absorption features at negative velocities for 1757−248. For comparison, Frail *et al.* (1993) have examined the absorption spectra of two nearby sources, the SNR W28 and the pulsar PSR 1758−23. For those two objects absorption extends up to +23 km s^{-1} and yields a kinematic distance of 3 kpc.

The absorption widths of the G 5.4−1.2 shell and G 5.27−0.9 are nearly identical. Both sources must be at least as far away as the distance corresponding to a radial velocity of +27 km s^{-1} and given the similarity of their absorption profiles we conclude that the G 5.4−1.2 and G 5.27−0.9 are likely at the same distance and are physically related.

It is difficult to assign a reliable kinematic distance to galactic objects in this direction (Frail & Weisberg 1990). In addition to velocity crowding at these longitudes, there is an apparent lack of cold H I gas ($T_b > 30$ K) beyond +30 km s^{-1}. The last significant absorption for *all* sources in this direction appears to be about +27 km s^{-1} even though the velocity at the tangent point extends to +200 km s^{-1}. Thus only a lower distance limit can be derived from these absorption profiles. Assuming a flat rotation curve (Fich *et al.* 1989), IAU 1985 constants ($\theta_0 = 220$ km s^{-1}, $R_0 = 8.5$ kpc), allowing for a ±7 km s^{-1} systematic deviation from pure circular rotation, we derive $d > 4.3$ kpc. By comparison, by using from the most recent Galactic electron density models (Taylor & Cordes 1993) the dispersion measure of PSR 1757−24 gives a distance of 4.6 kpc.

In summary, our H I absorption measurements give a lower limit distance to G 5.4−1.2 of 4.3 kpc, consistent with the dispersion measure based to the pulsar of 4.6 kpc (Taylor & Cordes 1993). Frail & Kulkarni (1991) used a distance of 6 kpc, determined from a lower quality H I absorption spectrum. Because our lower distance limit to G 5.4−1.2 so closely corresponds to the pulsar distance, the association seems firm. We favor a distance $d = 4.5$ kpc but we cannot rule out a larger distance for either PSR 1757−24 or G 5.4−1.2.

3.3 Spectral Index Distribution for G 5.4−1.2

Using the 20 cm continuum image from Becker & Helfand (1985) together with our own 327 MHz image, we are able to determine the spectral index distribution over the bright western arc of G 5.4−1.2. The 20 cm image is made from adding data from the CnB and DnC arrays. It was convolved to the resolution of the 327 MHz image and had a correction applied for the 30′ primary power pattern of the 25 m radio dishes (i.e., the field of view). The total flux density at 1465 MHz is 29 Jy, close to the value of 32 Jy determined from single dish measurements (Green 1991). The spectral index was calculated at each pixel by $\alpha = \log[I(1465\ \mathrm{MHz})/I(327\ \mathrm{MHz})]/\log[1465/327]$.

Figure 7 summarizes our results. There is considerable variation in the spectral index over G5.4−1.2, much of

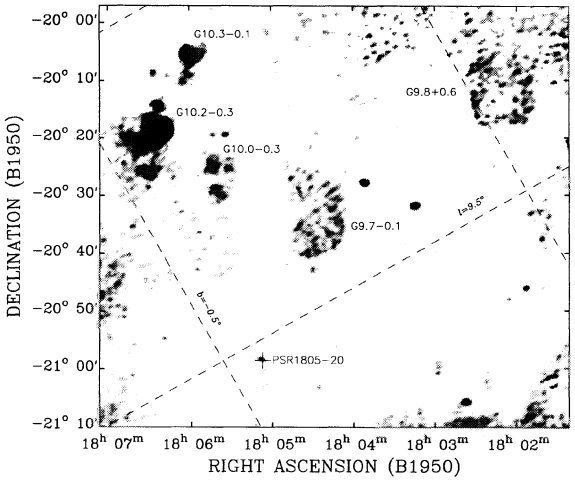

FIG. 5. A greyscale radio continuum image of the region surrounding a possible new supernova remnant G 9.7−0.1, just north of G 8.7−0.1. The two known SNRs (G 10.0−0.3 and G 9.8+0.6) and the two known H II regions (G 10.2−0.3 and G 10.3−0.1) are indicated, as well as a known pulsar PSR 1805−20.

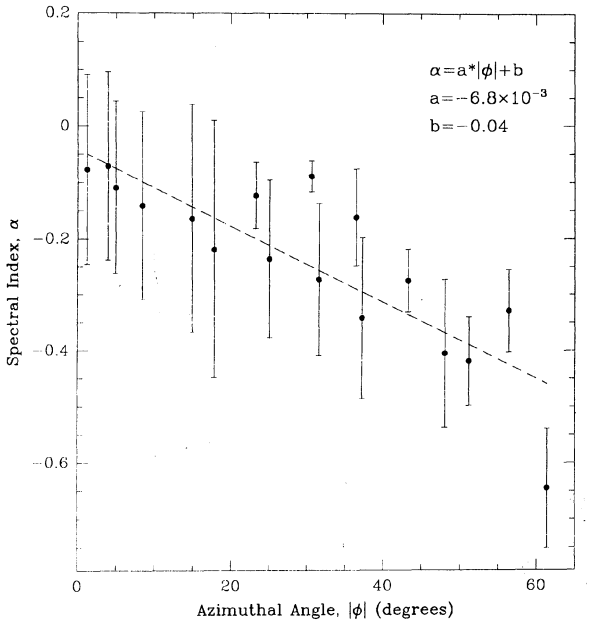

FIG. 7. The distribution of spectral index along the western side of G 5.4−1.2. The angle $|\phi|$ is defined as the angle along the SNR shell measured from the assumed explosion center (Sec. 4). The angle is zero where the neck of the duck meets the shell, and increases as one moves along the shell in either direction. A least squares fit to the data is shown as the solid line with its parameters given in the upper right corner.

which could be due to signal to noise. To reduce this we considered α only for those regions in which the 20 cm flux exceeds 200 mJy beam^{-1}. In addition, we formed a series of average α's in wedge-shaped regions, starting from the "center" of the remnant. We chose this center to be the point 5′ north of the geometric center, which intersects the line defined by the neck of the duck and the pulsar (see Sec. *3.1*). The parameter $|\phi|$ in Fig. 7 is the angle along the bright SNR shell measured from the center. The angle is zero where the neck of the duck meets the shell, and increases as one moves along the shell in either direction.

There is a clear trend in Fig. 7 of a steepening in the spectral index as a function of $|\phi|$. The trend is also apparent if one measures α at single points along the brightest part of the shell. It appears that the character of the SNR undergoes a transition from a flat spectrum plerionic remnant to a steep spectrum shell remnant along its western edge. This behavior was predicted by Frail & Kulkarni (1991). Evidently PSR 1757−24 is playing a prominent role in the energetics of the western shell of G 5.4−1.2, providing strong evidence for a real association between these two objects.

We caution that the datasets from which the spectral indices were calculated are not ideally matched. In particular, the 20 cm image may be missing some extended emission and the angular diameter of G 5.4−1.2 is larger than the field of view at 20 cm. A zero level offset due to missing extended flux at 1465 MHz would steepen the spectral index. This steepening would be more severe for the fainter parts of the remnant, which on average are located at larger values of $|\phi|$. We estimate that to produce the spectral index trend that we see in Fig. 7 would require nearly half of the total flux density of G 5.4−1.2 to have been missed by the interferometer at 1465 MHz (Green 1991), a value that is not supported by the total flux density measurements. Thus it appears that systematic errors alone cannot account this result, and until such time as a better high-frequency image is available, we accept that the trend is real.

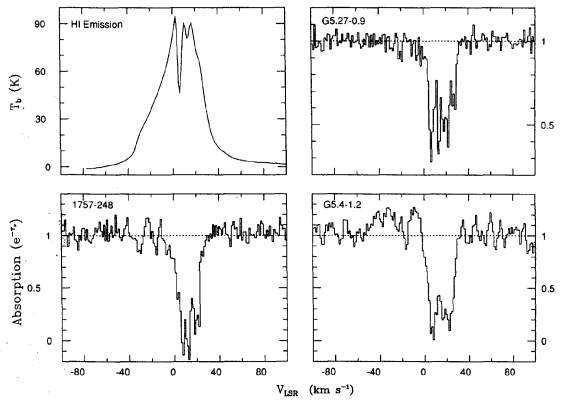

FIG. 6. Neutral hydrogen spectra. The emission spectrum in this direction (upper-left-hand panel) was formed by summing the total power of all 27 VLA antennas. The conversion to brightness temperature was made by scaling the peak of the data to agree with the value measured by Burton (1985), and assuming his conversion from antenna temperature to brightness temperature of 1.35. For the absorption spectra the name of each source is in the top left corner of each panel. Radial velocities (V_{LSR}) are measured with respect to the local standard of rest. The vertical axis is the fractional absorption, or $e^{-\tau_\nu}$, where τ_ν is the optical depth.

4. DISCUSSION

It is worthwhile to review the nature of these two possible PSR/SNR associations in the light of the new observations presented here.

SNR G 5.4−1.2 and PSR 1757−24. In addition to establishing that the H I absorption lower limit distance to G 5.4−1.2 agrees with the DM-based distance to PSR 1757−24, the most striking new evidence in favor of an association is the apparent steepening of the spectral index as one moves along the bright western shell of G 5.4−1.2, away from the point at which the pulsar is supposed to have penetrated the shell (Fig. 7). The "rejuvenation" model put forth by Shull *et al.* (1989) can be used to explain this behavior of $\alpha=\alpha(\phi)$.

Charged particles accelerated in the magnetosphere of a young pulsar will power a radio nebula with a spectral index between −0.1 and −0.3 (Reynolds 1988), consistent with the observational definition of a plerion (Weiler & Panagia 1978). On the other hand, the blast wave of a shell-type SNR will accelerate relativistic particles in the shocked transition zone between the shell and the ambient medium with a radio spectral index around −0.5 to −0.7 (Reynolds 1988). Thus it is the interaction between the plerionic emission, powered by the pulsar, and the shell emission, powered by the supernova shock, that produces the brighter, flatter spectrum emission on the western side of G 5.4−1.2 near the neck of the duck relative to the regions further away. The steepening spectral index at increasing values of $|\phi|$ reflects the weakening influence of the pulsar on the energetics of the shell, and the emergence of the underlying shock accelerated spectrum. While this may explain our observations in a qualitative sense, the details of the interaction remain an unsolved problem. In particular, the method of transport for the relativistic particles from the pulsar to the outlying areas of the shell is not obvious. Figure 7 contains important information on this issue, and we urge theoretical attention be given to the problem of particle and field transport in this class of "interacting composite" remnants.

In Sec. *3.1* we established that the shape G 5.4−1.2 was well described by a simple circle with a radius of 15.5′ and a center shown in Fig. 1. Admittedly, the remnant is poorly defined along its eastern half, but it does not show the breakout morphology of other SNRs such as 3C 391 (Reynolds & Moffett 1993) and VRO 42.05.01 (Pineault *et al.* 1987). An equally interesting point made in Sec. *3.1* was that the *implied* proper motion of PSR 1757−24 does not point back to the geometric center of the remnant. The simplest interpretation of this is that the pulsar was born elsewhere. Either we must accept that the association between PSR 1757−24 and G 5.4−1.2 is not real or else find an explanation for the offset.

Given the nonuniform nature of the interstellar medium, it is not too surprising that the geometric center of the remnant is offset from its true blast center (i.e., the birthplace of the pulsar). Caswell *et al.* (1987) suggested that the "lopsided" brightness of G 5.4−1.2 might be explained by either a gradient in the gas density or the magnetic field. A similar suggestion was made by Manchester *et al.* (1991), and in fact if the blast center were closer to the western edge of G 5.4−1.2 it would lower the required transverse velocity for PSR 1757−24. The exact location of the blast center is unknown, but it lies along a line defined by the position of the pulsar and the neck of the duck, with the distance of closest approach to the geometric center being 5′ north. To explore the possibility that the pulsar was born away from the geometric center and closer to the western edge of G 5.4−1.2 we considered a model where the SNR expands into an exponential gas layer with a density $n(z)$ and scale height h described by $n(z)=n_0\exp(-z/h)$. Lozinskaya (1992) presents a simple solution for the radius of a SNR as a function of θ, the polar angle defined relative to the direction of the density gradient:

$$R_s(\theta)=R_0\left(1+\frac{cR_0}{h}\cos\theta\right),$$

where R_0 is the radius of the SNR in the standard adiabatic solution ($n=n_0$) and $c=0.186$ is a constant. Figure 8 shows such a model for a vertical gradient with the blast center (large cross) offset from the geometric center (small cross) by 5′. Our model is parametrized by a quantity D, which is the separation of the blast center from the geometric center. The minimum value of D is 5′ and we require that the blast center lie along the line defined by motion of the pulsar (see above). Several fits to the data were made. While our model is simple and certainly not unique we achieve reasonable solutions for $D\leqslant 7'$, while for larger values of D the spheroid is too oblate to fit the image of G 5.4−1.2 in Fig. 1. Thus if the blast center is displaced

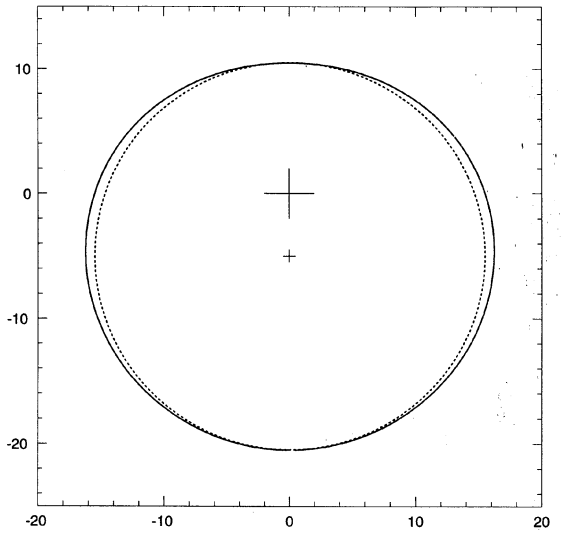

FIG. 8. The shape of a supernova remnant expanding into an exponential density gradient. The gradient runs north–south, decreasing towards the south. The small cross and dashed line are a circle fitting the observed remnant and its geometric center with a 15.5′ radius. The larger cross and the solid line show the blast origin and shape of a remnant expanding into a gas layer with an exponential scale height of 8.9′. The two crosses (geometric center vs blast center) are separated by 5′.

5′ to the north of the geometric center, it can be shifted as far as 4.5′ to the west without being inconsistent with the image of G 5.4−1.2. Again, while this is not a unique solution it is the farthest west we can shift the birthplace of the pulsar. A more complicated model, for example, taking into account the dynamical influence that PSR 1757−24 would have on the western side of G 5.4−1.2, is not warranted given the poorly defined edges of the remnant.

While we have established that the geometric and blast center of G 5.4−1.2 are not the same, the exact location of the blast center is not known. Model fitting constrains the blast center somewhat. The angular displacement of the pulsar from this blast center to its present location is between 16.1 and 20.6 arcmin; implying a proper motion for PSR 1757−24 of 63–80 milliarcsecond (mas) yr^{-1}, or a transverse velocity between 1300 and 1700 km s^{-1}. This value is closer to that derived by Manchester *et al.* (1991), but it is 30% below the value derived by Frail & Kulkarni (1991), principally because of our revision to the distance of G 5.4−1.2 (Sec. *3.2*). It is still unusually high and certainly larger than any space velocity yet measured for pulsars.

SNR G8.7−0.1 and PSR 1800−21. Our 327 MHz image of this remnant improves upon that made by Kassim & Weiler (1990b). Faint emission plumes are now visible breaking out along different parts of remnant, but there is no new extended emission seen in the vicinity of the pulsar. Thus PSR 1800−21 lies on the periphery of G 8.7−0.1, and provided that the blast center of the remnant is not far from the center given by Kassim & Weiler (1990b), the high transverse velocity of 1700 km s^{-1} inferred by Kassim & Weiler (1990a) is still required.

Unlike PSR 1757−24, this large required velocity presents some additional difficulty for the association between G 8.7−0.1 and PSR 1800−21. The bulk of the rotational energy loss $\dot{E}$ of a pulsar comes out as a relativistic pair-loaded wind which comes into equilibrium with the external pressure p_0 at a distance r_w from the pulsar. A standing shock will form at this point (Rees & Gunn 1974).

$$\frac{\dot{E}}{4\pi r_w^2 c}=p_0.$$

The external pressure acts to confine the flow. For a stationary pulsar in the ISM, the external pressure is small (3600 K $cm^{-3}=5\times10^{-13}$ erg cm^{-3}) and the resulting pulsar wind nebula is faint (Blandford *et al.* 1973). For a young pulsar like the Crab, still within the confines of its SNR, the synchrotron pressure can dominate (10^{-11} ergs cm^{-3}). An even more important source of confinement is the ram pressure due to a pulsar's motion through the ISM ($p_0=\rho v^2$). For PSR 1757−24 we estimate that $p_0=5\times10^{-8}\ n_0$, where n_0 is the ISM density in units of 1 cm^{-3}. The cometary nebula that surrounds PSR 1757−24 is a consequence of its large velocity and its high $\dot{E}$ (Frail & Kulkarni 1991). The lack of a similar structure around PSR 1800−21 implies that its space velocity is much lower and indicates a possible problem for this association.

Table 1 illustrates this point. In columns 2 and 3 the period and period derivative are given for both pulsars. All values are taken from the recent compilation of Taylor *et al.* (1993). The characteristic age ($\tau_c=P/2\dot{P}$), the surface dipole field ($B=10^{12}\sqrt{P\dot{P}}$), and the rotational energy loss rate ($\dot{E}=4\times10^{46}\dot{P}P^{-3}$) follow in the remaining columns. The physical parameters of these pulsars are amazingly similar; they are virtually interchangeable. However, the morphology and physical properties of the SNR in which they are associated are very different. PSR 1757−24 is surrounded by a compact, flat spectrum nebula (Frail & Kulkarni 1991) and it appears to be powering at least some of the radio emission of G 5.4−1.2. There is no similar evidence that PSR 1800−21 is energizing the surrounding medium and the radio spectrum of G 8.7−0.1 is −0.5 (Kassim & Weiler 1990b), a value typical of shell-type SNRs. If PSR 1800−21 is truly associated with G 8.7−0.1, it should have those same properties. Thus the absence of a pulsar wind nebula around PSR 1800−21 suggests that it is not a high velocity object and that it would not have been able to travel to its present position at the edge of G 8.7−0.1.

TABLE 1. Comparison of pulsar properties.

Pulsar (1)	P (s) (2)	$\dot{P}$ (10^{-15} s s^{-1}) (3)	Age (10^3 yrs) (4)	log B (G) (5)	log $\dot{E}$ (erg s^{-1}) (6)
1757−24	0.125	128	15	12.61	36.41
1800−21	0.134	134	16	12.63	36.35

Further questions can be raised about the validity of the association by comparing the emission and absorption profiles made against G 8.7−0.1 and PSR 1800−21. Kassim & Weiler (1990b) note that the radial velocities of the radio recombination lines from H II regions seen in absorption against G 8.7−0.1 are all within 5 km s^{-1} of each other, with a mean of 40 km s^{-1}. Similarly, they note that OH specta taken against G 8.7-0.1 show deep absorption up to velocities of 40 km s^{-1} Kassim & Weiler (1990a) derived a kinematic distance to G 8.7−0.1 of 5–6 kpc by using these H II regions seen in front (absorption) or behind (no absorption) G 8.7−0.1. The Lyne *et al.* (1985) model for the distribution of diffuse ionized gas in the Galaxy gave a DM-based distance for PSR 1800−21 of 5.3 kpc. The close similarity of these distances is one of the main reasons that Kassim & Weiler (1990a) suggested an association.

However, OH radial velocities for G 8.7−0.1 do not agree with the newer H I absorption results of PSR 1800−21 by Frail *et al.* (1991). Frail *et al.* saw the last absorption feature at 27 km s^{-1} and, in fact, assign an upper limit of 40 km s^{-1} on the basis of a *lack* of absorption, despite there being strong H I emission at this velocity. Based in part on the H I absorption results, the DM-based distance to PSR 1800−21 has now been changed to 3.9 kpc (Taylor & Cordes 1993). Thus it appears that PSR 1800−21 may be a foreground pulsar not associated with G 8.7−0.1.

5. CONCLUSIONS

We have imaged two supernova remnants at 327 MHz with the VLA, both of which are thought to be associated with young pulsars. Our observations have detected faint emission throughout G 5.4−1.2, and we have confirmed the existence of the faint eastern shell first noted by Caswell *et al.* (1987). Using H I absorption data, we have determined a lower distance limit to the SNR and we showed that this is consistent with the DM-based distance to PSR 1757−24. Another indication that this is a true pulsar-supernova remnant association comes from the distribution of radio spectral index (from 327 to 1465 MHz) across the bright western side of G 5.4−1.2. A steepening in the spectral index is seen away from the point at which the pulsar is thought to have penetrated the shell. This result awaits confirmation with better-quality data at higher frequencies.

We show that the geometric center of the remnant is probably not the point of origin of the supernova event that gave birth to PSR 1757−24 and we have explored models for the evolution of SNRs in exponential gas layers, to solve for a range of possible distances that the pulsar could have been born away from the geometric center and still have produced a remnant whose shape is consistent with the radio image. These models constrain the range of possible transverse velocities to be 1300–1700 km s^{-1}. Lowering the velocity (and thus moving the pulsar's birthplace close to the western edge) results in a morphology that is inconsistent with the near circular shape of G 5.4−1.2.

For G 8.7−0.1 the new 327 MHz radio continuum image reveals previously undetected faint structure in the remnant but there is little new extended emission around PSR 1800−21. There also appear to be several new difficulties in accepting a physical association first proposed by Kassim & Weiler (1990a). We note that the similarities between PSR 1757−24 and PSR 1800−21 contrast sharply with the dissimilarities between G 5.4−1.2 and G 8.7−0.1 and suggest that PSR 1800−21 is *not* a high velocity object and is probably not associated with G 8.7−0.1. New absorption data suggest that PSR 1800−21 lies 1–2 kpc in front of G 8.7−0.1.

Proper motion measurements of both pulsars are still required to test our conclusions. In the case of PSR 1757−24 we expect a proper motion of 63–80 mas yr^{-1} nearly due west, while for PSR 1800−21 we expect approximately 8 mas yr^{-1} (assuming a typical pulsar velocity of 150 km s^{-1}) in a random direction. Observations which are planned or currently underway will be able to measure such motions in a few years.

We would like to thank Tim Cornwell for developing the imaging algorithms which made this project possible. D.A.F. thanks Bob Becker for making his 20 cm image of G 5.4−1.2 available and K. Dwarakanath for his willingness to comment and criticize on all aspects of this work. Basic research in Radio Interferometry at the Naval Research Laboratory is supported by the Office of Naval Research through Funding Document No. N00014-93-WX-35012, under NRL work unit 2567.

REFERENCES

Abramovici, A., *et al.* 1992, Science, 256, 325
Bailes, M., & Johnston, S. 1993 in Review of Radio Science (URSI), edited by W. Ross Stone (Oxford University Press, London), p. 677
Becker, R. H., & Helfand, D. J. 1985, Nature, 313, 118
Blandford, R. D., Ostriker, J. P., Pacini, F., & Rees, M. J. 1973, A&A, 23, 145
Burrows, A., & Fryxell, B. A. 1992, Science, 258, 430
Burton, W. B. 1985, A&AS, 62, 365
Caswell, J. L. 1983, MNRAS, 204, 833
Caswell, J. L., Kesteven, M. J., Komesaroff, M. M., Haynes, R. F., Milne, D. K., Stewart, R. T., & Wilson, S. G. 1987, MNRAS, 225, 329
Cornwell, T. J. 1993, VLA Scientific Memo No. 164, NRAO
Cornwell, T. J., & Perley, R. A. 1992, A&A, 261, 353
Cornwell, T. J., Uson, J. M., & Haddad, N. 1992, A&A, 258, 583
Dewey, R. J., & Cordes, J. M. 1987, ApJ, 321, 780
Fich, M., Blitz, L., & Stark, A. A. 1989, ApJ, 342, 272
Frail, D. A., & Clifton, T. R. 1989, ApJ, 336, 854
Frail, D. A., Cordes, J. M., Hankins, T. H., & Weisberg, J. M. 1991, ApJ, 382, 168
Frail, D. A., & Kulkarni, S. R. 1991, Nature, 353, 785
Frail, D. A., Kulkarni, S. R., & Vasisht, G. 1993, Nature (in press)
Frail, D. A., & Weisberg, J. M. 1990, AJ, 100, 743
Green, D. A. 1991, PASP, 103, 209
Harrison, P. A., Lyne, A. G., & Anderson, B. 1993, MNRAS, 261, 113
Haslam, C. G. T., Salter, C. J., Stoffel, H., & Wilson, W. E. 1982, A&AS, 47,1
Helfand, D. J., & Becker, R. H. 1985, Nature, 313, 118
Kassim, N. E. 1991, AJ, 103, 943
Kassim, N. E., & Weiler, K. W. 1990a, Nature, 343, 146
Kassim, N. E., & Weiler, K. W. 1990b, ApJ, 360, 184
Lozinskaya, T. A. 1992, Supernovae and Stellar Wind in the Interstellar Medium (AIP, New York)
Lyne, A. G., Anderson, B., & Salter, M. J. 1982, MNRAS, 201, 503
Lyne, A. G., Manchester, R. N., & Taylor, J. H. 1985, MNRAS, 213, 613
Manchester, R. N., D'Amico, N., & Tuohy, I. R. 1985, MNRAS, 212, 975
Manchester, R. N., Kaspi, V. M., Johnston, A. G., Lyne, A. G., & D'Amico, N. 1991, MNRAS, 253, 7
Odegard, N. 1986, AJ, 92, 1372
Pineault, S., Landecker, T. L., & Routledge, D. 1987, ApJ, 315, 580
Rees, M. J., & Gunn, J. E. 1974, MNRAS, 167, 1
Reynolds, S. P. 1988, in Galactic and Extragalactic Radio Astronomy, edited by G. L. Verschuur and K. I. Kellermann (Springer, Berlin), p. 439
Reynolds, S. P., & Moffett, D. A. 1993, AJ, 105, 2226
Shull, J. M., Fesen, R. A., & Saken, J. M. 1989, ApJ, 346, 860
Taylor, A. R., Wallace, B. J., & Goss, W. M. 1992, AJ, 103, 931
Taylor, J. H., & Cordes, J. M. 1993, ApJ, 411, 674
Taylor, J. H., Manchester, R. N., & Lyne, A. G. 1993, preprint
Weiler, K. W., & Panagia, N. 1978, A&A, 70, 419
Weiler, K. W., & Sramek, R. A. 1988, ARA&A, 26, 295
Woosley, S. E. 1987, in The Origin and Evolution of Neutron Stars, IAU Symposium No. 125, edited by D. J. Helfand and J. -H. Huang (Reidel, Dordrecht), p. 255

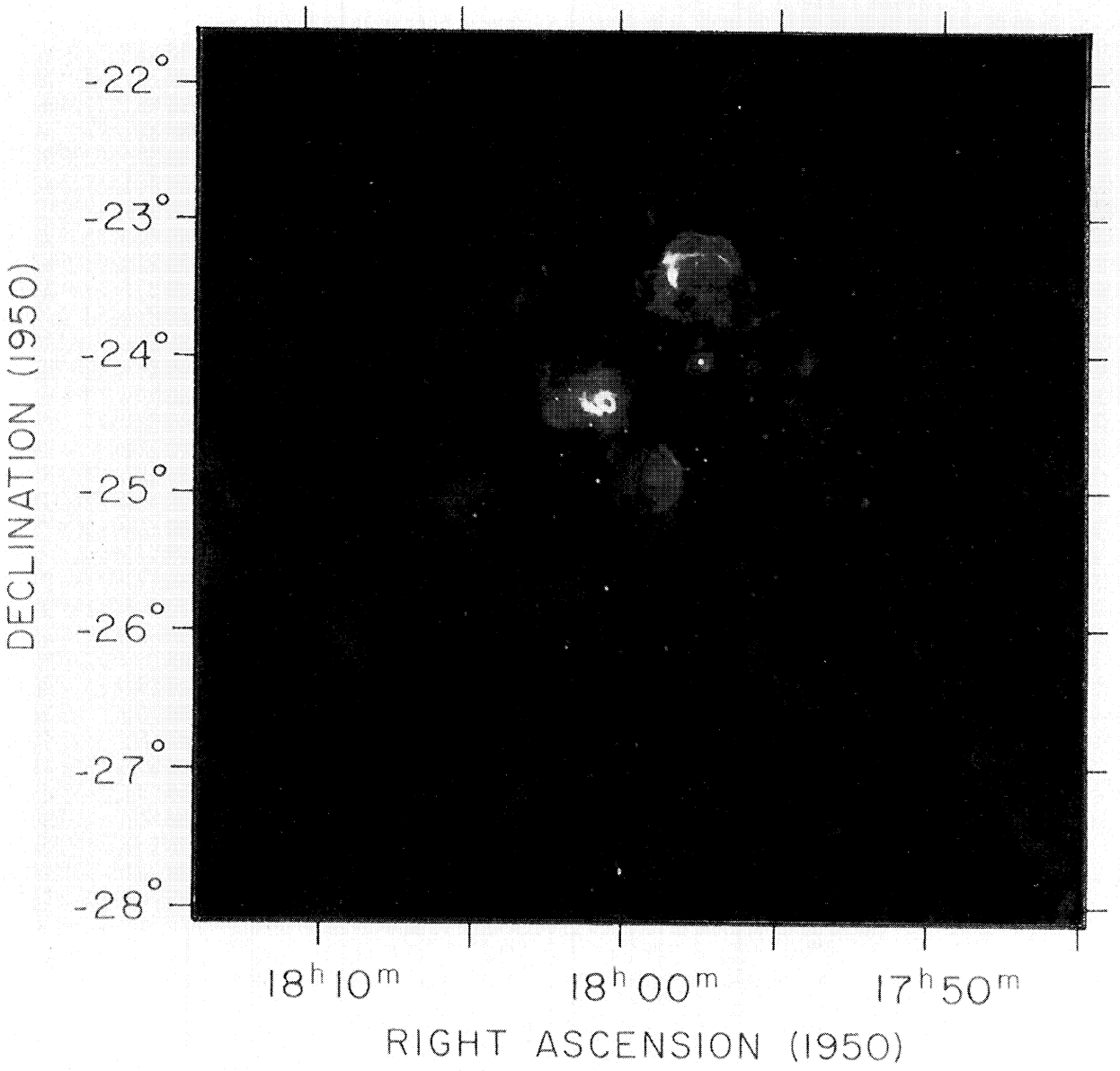

FIG. 2. A radio continuum image of the region centered on the supernova remnant G 5.4−1.2 at 327 MHz. The image parameters are the same as those in Fig. 1 but now the full field of view is visible. Numerous radio sources are visible, including the H II regions M 8 and W 28A and the SNR W 28.

Frail *et al.* (see page 1122)

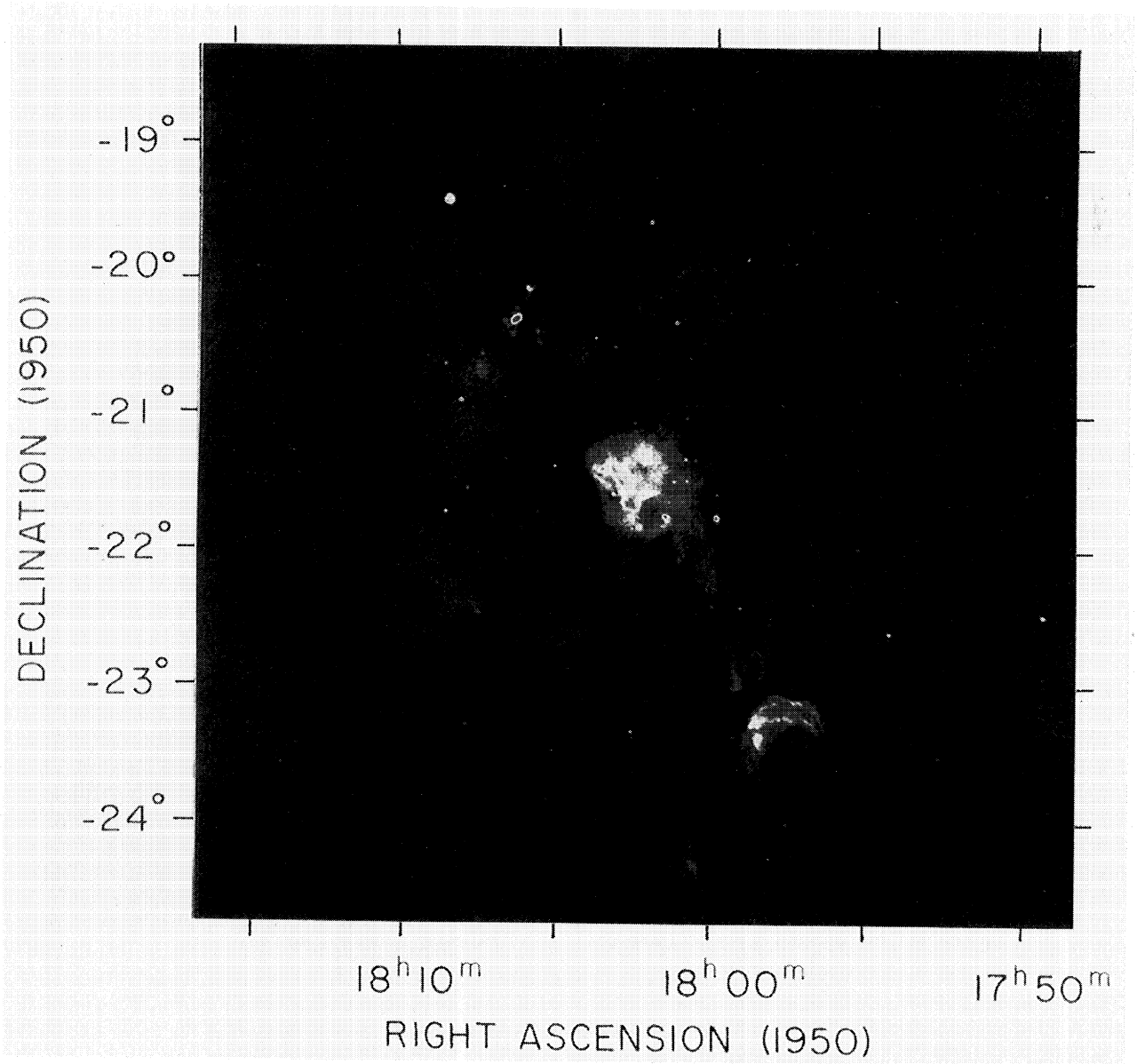

FIG. 4. A radio continuum image of the region centered on the supernova remnant G 8.7−0.1 at 327 MHz. The image parameters are the same as those in Fig. 2.

Frail *et al.* (see page 1123)